

Relaxation and rocking-curve broadening of strained (Ga,In)As single layers on (001) GaAs

C. R. Wie

State University of New York at Buffalo, Department of Electrical and Computer Engineering,
Bonner Hall, Amherst, New York 14260

(Received 23 May 1988; accepted for publication 29 November 1988)

We have measured the lattice relaxation of various strained $\text{Ga}_{1-x}\text{In}_x\text{As}$ layers which are thicker than the equilibrium critical thickness. Samples with a thickness near the energy balance model critical thickness exhibited a large relaxation. We have analyzed the strain relaxation data in a GaInAs/GaAs system using the Dodson-Tsao plastic flow model [Appl. Phys. Lett. **52**, 852 (1988)]. It was found that the model provides a reasonably good fit to the data, however, the model parameters have widely different values for the GaInAs/GaAs samples with different mismatches. One parameter of the model shows an approximate inverse-square-law dependence on the misfit. The rocking-curve linewidths are presented for the GaInAs layers. The measured linewidths are discussed in terms of the theoretical linewidth, dynamical x-ray diffraction, and defect density depth distribution.

I. INTRODUCTION

Lattice relaxation of strained epitaxial layers which are thicker than the equilibrium critical thickness has been a subject of several recent publications.¹⁻⁴ Most of these reports have focused on correct determination of the critical layer thickness (CLT), experimentally^{1,2} or theoretically.^{3,4} The experimental data obtained using techniques insensitive to a low dislocation density [such as x-ray rocking-curve (XRC) and Raman techniques] indicated that the apparent CLTs are greater than the equilibrium CLTs.^{5,6} In an attempt to resolve the discrepancies in various experimental data, Fritz² argued that the finite resolution of the experimental technique causes measured CLTs to be greater than the equilibrium CLTs.⁷ The experimental data obtained using techniques sensitive to a very low dislocation density (such as photoluminescence microscopy^{1,8} and low-temperature Hall measurements⁹) agreed with the Matthews' equilibrium theory, showing the onset of dislocation generation at a thickness close to the equilibrium CLT. Although insensitive to a low dislocation density, the XRC technique is capable of measuring the lattice relaxation when the relaxation is sufficiently high (greater than 10^{-4}). In this paper, we present the experimental data on lattice relaxation and on rocking-curve broadening of single $\text{Ga}_{1-x}\text{In}_x\text{As}$ layers on GaAs(001) substrates. We apply to the strain relaxation data the nonequilibrium model of strain relaxation which was recently introduced by Dodson and Tsao.³

II. EXPERIMENT

The GaInAs layers were grown at 550 °C by molecular-beam epitaxy (MBE) or at 650 °C by metalorganic chemical vapor deposition (MOCVD). All the GaInAs layers were grown on (001) face GaAs substrates. The GaInAs layers were grown on a GaAs buffer layer except for the thickest layer (about 7 μm) which was grown on a 0.8-μm strained layer superlattice (SLS) buffer. A double-crystal x-ray rocking-curve system, equipped with a conventional copper x-

ray tube, was used for the measurements. The [001] lattice spacings were obtained, relative to the substrate, from the two symmetric 004 rocking curves which differed in the azimuthal angle by 180° with respect to the surface normal. The in-plane lattice spacings, in the two (110) directions, were measured from the four 224 rocking curves.¹⁰ The measured lattice spacings can be written as $\epsilon_{ijk}^x = (d_{ijk} - d_s)/d_s$, where d_{ijk} is the lattice spacing of the (ijk) planes of the deformed GaInAs crystal, d_s is the (ijk) lattice spacing of the undeformed GaAs substrate, and the ϵ_{ijk}^x is the so-called x-ray strain. Using the rocking-curve technique, the in-plane lattice mismatch ϵ_{110}^x can be obtained if it is greater than 0.01%. This minimum lattice mismatch corresponds to an average spacing of 2 μm or an average density of 5000/cm for the 60° misfit dislocations. In this paper, the strained layers, which have an in-plane mismatch of less than 0.01%, are referred to as pseudomorphic layers.

The bulk-equivalent lattice constant, a_f , for the film or the misfit, ϵ_f , can be calculated from the x-ray strains using the linear elasticity theory,

$$\epsilon_f = (a_f - a_s)/a_s \\ = [v\epsilon_{110}^x + v\epsilon_{\bar{1}\bar{1}0}^x + (1-v)\epsilon_{001}^x]/(1+v), \quad (1)$$

where a_s is the substrate lattice constant and v is the Poisson ratio for the film. The indium content x in the $\text{Ga}_{1-x}\text{In}_x\text{As}$ film can be obtained from the film lattice constant a_f of Eq. (1) using Vegard's law. The indium content x estimated in this way tends to be smaller than the nominal indium content or the x value obtained using other techniques such as energy-dispersive x-ray analysis.¹⁰ The underestimation of x in the rocking-curve technique is roughly 0.01–0.03 for a sample with $x \leq 0.2$ and a thickness of 400 Å–7 μm. Perhaps this is because of a difference in the elastic properties (such as the Poisson ratio) between the thin-film and the bulk semiconductors. However, according to our experience, the lattice relaxation never exceeds the ϵ_f obtained from Eq. (1). Hence we use the x value estimated from Eq. (1) when plotting the relaxation data.

III. STRAIN RELAXATION OF $\text{Ga}_{1-x}\text{In}_x\text{As}/\text{GaAs}$

The lattice relaxation is defined as

$$R \equiv (a_{\parallel} - a_s) / (a_f - a_s) = (\epsilon_{\parallel}^{xr} / \epsilon_f) 100\%, \quad (2)$$

where a_{\parallel} is the film lattice constant in the [100] direction in the sample plane and $\epsilon_{\parallel}^{xr}$ is the average in-plane mismatch $(\epsilon_{110}^{xr} + \epsilon_{\bar{1}\bar{1}0}^{xr})/2$. R is zero for a pseudomorphic layer and 1 for a completely relaxed layer. In Fig. 1, we plot the layer thickness¹¹ as a function of layer composition which is in turn calculated from the x-ray data. The "x" data symbols represent the MBE-grown samples and the "y" data symbols represent the MOCVD-grown samples. The number given for each data point is the relaxation R in percent. In Fig. 1, the four "x" data points without any number had the in-plane mismatch $\epsilon_{\parallel}^{xr}$ less than 0.01%. Figure 1 shows the equilibrium CLT, curve d is calculated from the equilibrium theory⁷ using the anisotropic elastic moduli, and curve a is calculated from the energy balance model of People and Bean.¹² Curves b and c in Fig. 1 will be discussed later. It is seen in Fig. 1 that a substantial relaxation (10%–60%) occurs below the critical thickness given by the energy balance model. For samples thicker than the energy balance model critical thickness, the relaxation approaches 70%–100%.

It is not difficult to understand the role of the energy balance model critical thickness in the lattice relaxation process from the basic assumptions made in the original derivation.¹² The assumption was that the areal density of the strain energy equals, at the critical thickness, the areal density of the dislocation energy. As pointed out by Dodson *et al.*,⁴ the strain energy will be sufficient to nucleate dislocations everywhere if the energy density is high enough to nucleate dislocations locally. This implies that a major lattice relaxation shall occur at a thickness near the energy balance model CLT, which we observe in Fig. 1. This, along with the low sensitivity of the XRC technique in measuring the change in $\epsilon_{\parallel}^{xr}$ (minimum 10^{-4}), may be the reason behind the observation by Orders and Usher that the XRC-measured

critical thickness was consistent with the energy balance model.⁵

Recently, there has been a rapid advancement in understanding the structural relaxation in strained-layer structures.^{3,16} The nonequilibrium model,³ recently introduced by Dodson and Tsao based on the plastic flow driven by the excess stress in the strained layer, successfully explained the strain relaxation data for SiGe/Si of Bean *et al.*¹⁷ and of Kasper, Herzog, and Kibbel.¹⁸ We shall apply the Dodson–Tsao plastic flow model to our data.

First, we briefly outline the Dodson–Tsao plastic flow model. In their model, the time dependence of strain relief γ is described by a nonlinear ordinary differential equation

$$\frac{d\gamma(t)}{dt} = C \left(\frac{\sigma_{ex}}{\mu} \right)^2 [\gamma(t) + \gamma_0], \quad (3)$$

where C is a constant to be determined by fitting Eq. (3) to the experimental data, μ is the shear modulus, γ_0 represents a source term for misfit dislocation, and σ_{ex} is the excess stress which is the driving force of the strain relaxation. Equation (3) is based on the Alexander–Hassen model for plastic deformation in bulk semiconductors.¹⁹ The right-hand side of Eq. (3) includes both the kinetics of dislocation motion and the increase of dislocation density via dislocation multiplication. The excess stress σ_{ex} for a single strained overlayer is

$$\sigma_{ex} = 2\mu[(1 + \nu)\epsilon/(1 - \nu) - (1 - \nu \cos^2 \beta) \times \ln(4h/b)/4\pi(1 - \nu)(h/b)], \quad (4)$$

where ν is the Poisson's ratio, ϵ is the (instantaneous) unrelied portion of strain which equals $\epsilon_f - \gamma(t)$, β is the angle between the dislocation line and the Burgers vector, b is the magnitude of the Burgers vector, and h is the thickness of the strained overlayer. The strain relief $\gamma(t)$ in the Dodson–Tsao model is identified as the average in-plane mismatch $\epsilon_{\parallel}^{xr}$ in our data.

Second, our strain relaxation data in Fig. 1 need to be converted to an equivalent data set, corresponding to a single composition. This is because the fit quality may be best judged by plotting the theoretical and experimental data as a function of layer thickness for a given composition. We converted the MBE-sample data, which have x values between 0.07 and 0.11 in Fig. 1, to the equivalent in-plane mismatch $\epsilon_{\parallel}^{xr} = R\epsilon_f$ by using the values for R which are given in Fig. 1 and using the value of ϵ_f which is calculated for the x value of 0.095 for $\text{Ga}_{1-x}\text{In}_x\text{As}/\text{GaAs}$ using Vegard's law. The resulting in-plane mismatches are plotted as "x" in Fig. 2 as a function of the layer thickness.

Third, the in-plane mismatch data (or the strain relief data) are fit with Eq. (3) by numerically integrating the equation. Figure 2 shows the best fit to the data, which occurred when the fitting parameters, C and γ_0 , were approximately 25 and 1.1×10^{-10} , respectively. These parameters were varied over 3.4–3400 for C , and 3×10^{-5} – 9×10^{-45} for γ_0 , until the best fit was obtained. The dislocation source term, γ_0 , from the fit is reasonably small, being smaller than any relaxation observed in the experiments. The constant C , however, appears to be too small in view of an appropriate bulk value.²⁰ Apart from the small value of the phenomeno-

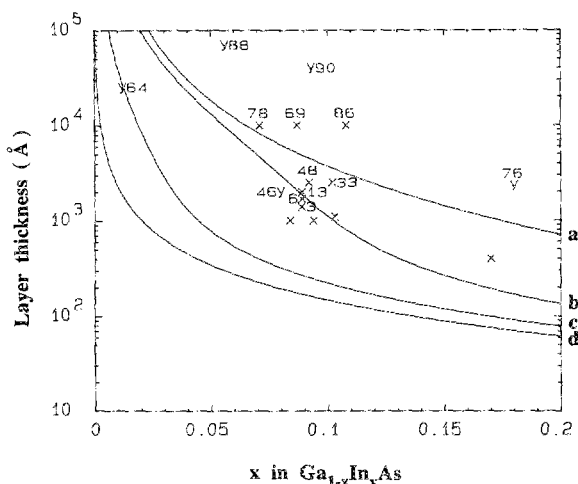


FIG. 1. Curve d is the equilibrium critical thickness and curve a is the energy balance model critical thickness. The "x" symbols are data points for the MBE-grown samples and the "y" symbols are for MOCVD-grown samples. The number near each data point is the lattice relaxation given by Eq. (2). Curves b and c are the Dodson–Tsao critical thicknesses at 550 and 650 °C, respectively.

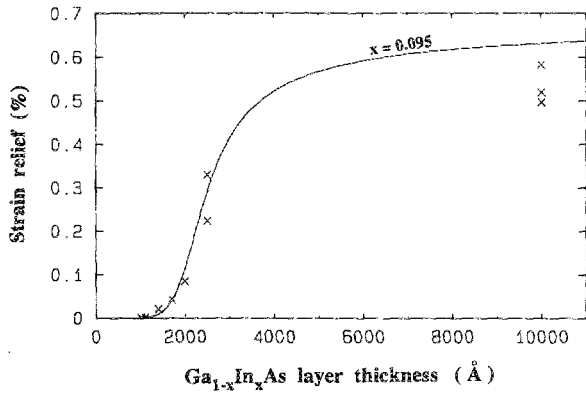


FIG. 2. Strain relief (or in-plane mismatch) vs $\text{Ga}_{1-x}\text{In}_x\text{As}$ layer thickness. The solid curve is a calculation using Eq. (3) with $C = 25$ and $\gamma_0 = 1.1 \times 10^{-10}$ for $x = 0.095$. Data points are the MBE sample data with $x = 0.07-0.11$ which are converted to an equivalent relaxation corresponding to $x = 0.095$.

logical constant C , the Dodson-Tsao plastic flow model gives a good fit to the experimental data for the layer thicknesses up to 2500 Å.

Finally, curves b and c in Fig. 1 are predictions of the Dodson-Tsao model for the critical thickness which would be observed in the $\text{Ga}_{1-x}\text{In}_x\text{As}/\text{GaAs}(100)$ system, given an experimental sensitivity to the strain relief of 10^{-4} for the rocking-curve technique. Curve b in Fig. 1 is a calculation, based on Eq. (3) with $C = 25$ and $\gamma_0 = 1.1 \times 10^{-10}$, of the observable critical thickness for the MBE samples which were grown at a substrate temperature of 550 °C. Curve c is a similar calculation for the MOCVD samples grown at 650 °C, taking into account the temperature dependence, $\exp(-U/kT)$, for C^{19} and assuming $U = 1.62$ eV as the activation energy of dislocation glide in GaAs. Curve b fits reasonably to the MBE data points ("x" symbols) in the neighborhood of $x = 0.1$. Curve c is not directly comparable to the MOCVD data points.

However, from Figs. 1 and 2 and from calculations of the strain relief for each data point in Fig. 1, the following features could be observed: (1) The calculated strain relief agrees reasonably well with the data in Fig. 1, except for the high mismatch ($x = 0.17$), small thickness ($h = 400$ Å) MBE sample and the low mismatch ($x = 0.012$), large thickness ($h = 2.5$ μm) MOCVD sample. (2) For the former, Eq. (3) drastically overestimates the strain relief (calculated 8×10^{-3} , measured $< 10^{-4}$), and for the latter, it drastically underestimates the strain relief (calculated 2.3×10^{-5} , measured 5.5×10^{-4}), which are also implied in Fig. 1 by the critical thickness curves b and c. (3) For samples thicker than 0.5 μm (except for the already mentioned MOCVD sample), Eq. (3) consistently predicts the strain relief, which is higher than the experimental results, but agrees within 3%–20%. (4) Figure 2 shows that the strain relief for the GaInAs/GaAs system (misfit $\approx 0.7\%$) increases rapidly in the thickness range of 1500–3500 Å, whereas the $\text{Si}_{0.5}\text{Ge}_{0.5}/\text{Si}$ system (misfit $\approx 2\%$) shows a rapid increase in the thickness range 100–500 Å (see Ref. 3). The above observations appear to indicate that the phenomenological parameters, C and γ_0 , may assume very different

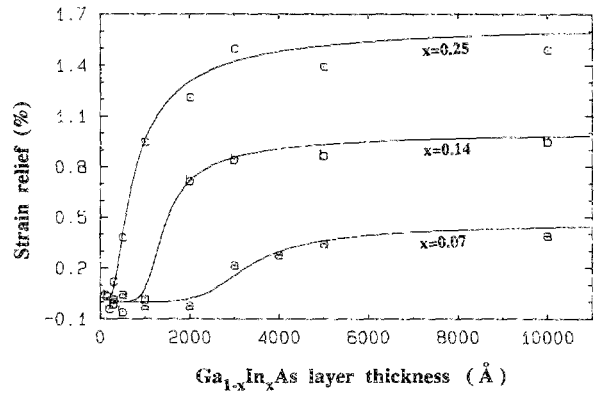


FIG. 3. The fit of the Dodson-Tsao plastic flow model [Eq. (3)] to the strain relief data, plotted as "a" for $x = 0.07$, as "b" for $x = 0.14$, and as "c" for $x = 0.25$. The strain relief data are calculated from the perpendicular lattice constants of Orders and Usher (Ref. 5).

values for different lattice mismatches, even for samples grown under similar conditions. Even though this conclusion is tentative and needs further investigation, it may have important implications in interpreting the parameters C and γ_0 (as in the recent publication by Dodson¹⁶) and in understanding the dynamics of strain relaxation.

The above conclusion is reinforced by the results of fitting Eq. (3) to the data by Orders and Usher.⁵ Figure 3 shows the fit of the three different data sets with $x = 0.07$, 0.14, and 0.25 for $\text{Ga}_{1-x}\text{In}_x\text{As}/\text{GaAs}$ which was grown at a substrate temperature of 530 °C and at a growth rate of about 3 Å/s. The parameter values, C and γ_0 , are 25.2, 5×10^{-8} for $x = 0.07$, 11.1, 3×10^{-10} for $x = 0.14$, and 2.72, 1.5×10^{-6} for $x = 0.25$, respectively. Thus, the fitting parameter values are widely different for the GaInAs/GaAs system with different misfits. Figure 4 shows a plot of C as a function of the misfit ϵ_f . Figure 4 shows that the parameter C is approximately proportional to ϵ_f^{-2} . It is interesting to note that the parameter C for $\text{Si}_{0.5}\text{Ge}_{0.5}/\text{Si}$ also agrees with this dependence. Without an attempt to explain this dependence, we tentatively conclude that the more appropriate model parameter is C_1 , where

$$C = C_1 \epsilon_f^{-2}. \quad (5)$$

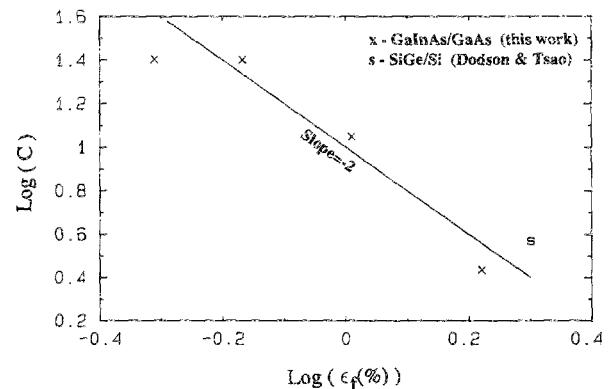


FIG. 4. Plot of the fitting parameter C as a function of the lattice misfit ϵ_f . The data were obtained from fitting Eq. (3) to the strain relief data for the GaInAs/GaAs system (x) and from Ref. 3 for the $\text{Si}_{0.5}\text{Ge}_{0.5}/\text{Si}$ system (s). The solid line indicates that C is proportional to ϵ_f^{-2} .

IV. ROCKING-CURVE BROADENING

We have also measured the rocking-curve FWHM (full width at half maximum) for the layers at various relaxation states and compared them against the theoretical linewidths calculated using the dynamical x-ray diffraction theory. Figure 5 shows, as vertical bars, the rocking-curve FWHMs measured from the symmetric 004 rocking curves. The thin vertical bars represent the MBE-grown samples and the thicker bars represent the MOCVD-grown samples. The solid curve is the calculated FWHM. The experimental FWHMs are for x values of $\text{Ga}_{1-x}\text{In}_x\text{As}$ ranging from 0.05 to 0.18. Figure 5 also shows the FWHM data of Kamigaki *et al.*¹³ as k and that of Orders *et al.*⁵ as r . The number near each data point is the in-plane mismatch in units of 10^{-4} . Data points without any number have a strain relaxation below the XRC sensitivity limit. Figure 5 shows that the experimental FWHM increases by a factor greater than 2 as the film relaxes from the pseudomorphic state. However, as discussed in the previous section, this increase in FWHM is not a sign of the onset of misfit dislocation generation (or the initial strain relaxation), but rather a sign of a major strain relaxation. The measured linewidths initially increase with thickness, reflecting the deteriorating crystal quality near the interface as the layer-strain relaxes further. However, for samples thicker than about $1\ \mu\text{m}$, the linewidths become less sensitive to the quality of the near-interface region, as Fig. 5 indicates. The MOCVD-grown samples (represented by the thicker bars in Fig. 5) had relatively poor layer qualities, which were observed from the Nomarski micrographs¹⁰ and from the cross-section transmission electron micrographs (XTEM). These MOCVD layers have different buffer layers¹⁰ and exhibit the poor layer qualities by the relatively large FWHM (see Fig. 5) for a small strain relaxation and a large thickness.

An important point of Fig. 4 is that, for samples with a strain relaxation less than the XRC sensitivity limit (10^{-4}), the rocking-curve linewidth is close to the theoretical linewidth of the ideal crystal. In other words, the crystal quality in the near-interface region is as good as the perfectly lattice-matched layer as far as the rocking-curve technique can see. The theoretical curve showing the monotonically decreasing linewidth with thickness is a result of the dynamical x-ray diffraction. For a thickness below $0.3\ \mu\text{m}$, the experimental linewidth scales approximately with the in-plane mismatch (see Fig. 5). For thicker layers, the linewidth at a given thickness is greater for a higher in-plane mismatch; at a similar mismatch, it is smaller for thicker films (the MOCVD samples do not follow this trend because of the poor growth quality). As a measure of the crystal quality in lattice-mismatched epitaxial layers, the rocking-curve FWHM depends on two aspects which are discussed below.

First, in the rocking curves, the x-ray intensity diffracted from different depths is weighted, due to the normal absorption and extinction. For layers thinner than $\sim 3000\ \text{\AA}$, the kinematical x-ray diffraction theory is a good approximation to the dynamical theory for the GaAs crystals with $\text{CuK}\alpha_1$ radiation.²¹ If extinction is ignored and only the normal absorption is considered in the kinematical diffraction theory, the weighting effect in the x-ray intensity from differ-

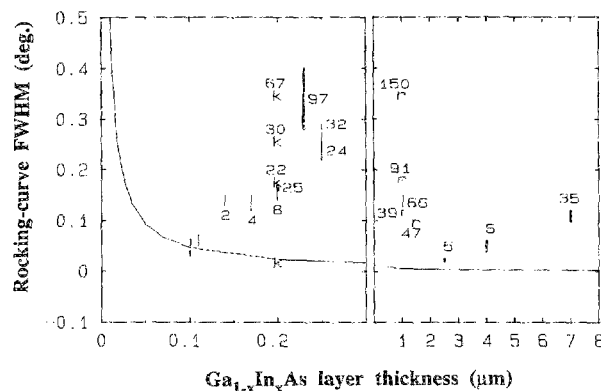


FIG. 5. The rocking-curve broadening is plotted as a function of the $\text{Ga}_{1-x}\text{In}_x\text{As}$ layer thickness. The thin bars are the MBE-grown samples and the thicker bars are the MOCVD-grown samples. The solid curve is the FWHM calculated using the Eq. (5) for an ideal crystal. Also plotted as "k" are Kamigaki's data (Ref. 15) and as "r" are Orders' data (Ref. 5). The number near each data point is the strain relief in units of 10^{-4} .

ent depths is nearly uniform for layers thinner than $0.3\ \mu\text{m}$, because the absorption length is about $29\ \mu\text{m}$. Therefore, the rocking-curve linewidth should scale with ϵ_{\parallel}^2 for these thin layers (if the growth technique is the same). Figure 5 shows that the linewidth increases with an increasing in-plane mismatch. For layers thicker than $\sim 3000\ \text{\AA}$, the weighting effect in the reflected x-ray intensity (originating from different depth) is stronger because extinction plays an increasingly important role in the diffraction process.

Second, the defect density caused by the lattice relaxation decreases as the distance from the interface increases. The XTEM micrographs of some of the samples studied here showed a decreasing line defect density as the distance from the interface increased. Other XTEM work on GaAs/Si heteroepitaxial samples showed a sharply decreasing line defect density as the distance from the GaAs/Si interface increased (on the order of $1\ \mu\text{m}$). In addition, there is evidence that the dislocation density in epitaxial GaAs decreases at a faster rate in strained epitaxial layers than in unstrained homoepitaxial layers.²² Therefore, the defect density distribution in the lattice-relaxed strained epitaxial layers and the weighting effect in the reflected x-ray intensity due to the dynamical diffraction will determine the rocking-curve linewidth observed for the thicker layers in Fig. 5 (i.e., films thicker than $1\ \mu\text{m}$). For the thick films, the linewidth at a given mismatch will increase with an increasing in-plane mismatch and the linewidth at a given in-plane mismatch will decrease with an increasing layer thickness. Dependence of the ideal crystal FWHM on the layer thickness is significant only for layers thinner than about $1000\ \text{\AA}$ as the solid curve in Fig. 5 shows.

Last, we briefly discuss the substrate effect in the rocking-curve FWHM. The plane-wave solution to the Takagi-Taupin equation¹⁴ for a single-crystal plate is

$$X = -iB \tan(sA) / [s - iC \tan(sA)], \quad (6)$$

where the sample is a (001) face cubic crystal, X = the scattering amplitude,

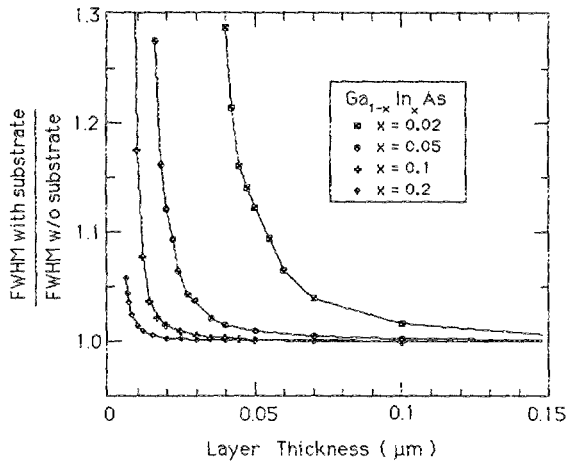


FIG. 6. The ratio of rocking-curve FWHMs for a layer with and without a substrate. The increase at the small thickness is due to the overlap of the two reflected amplitudes from the layer and the substrate.

$$\begin{aligned}
 B &= 1 + ik, \quad C = y + ig, \\
 s &= \sqrt{(C^2 - B^2)}, \quad k = F''_H / F'_H, \\
 g &= -F''_0 / F'_H, \quad F_{0,H} = F'_{0,H} + iF''_{0,H}, \\
 A &= r_e \lambda F'_H t / (V_c \sin \Theta_B), \\
 y &= [\pi V_c \sin(2\Theta_B) (\Delta\Theta + C_1 \epsilon_{001}^x + C_2 \epsilon_{110}^x + g)] / \\
 &\quad (\lambda^2 r_e F'_H),
 \end{aligned}$$

$F_{0,H}$ is the structure factor for the incident and diffracted beams, $r_e = 2.814 \times 10^{-5} \text{ \AA}$, t is the film thickness, V_c is the unit cell volume, $C_{1,2}$ is the geometrical constant,¹⁵ Θ_B is the Bragg angle, and $|X|^2$ is the reflecting power of the crystal plate. Equation (6) was obtained by letting the substrate scattering amplitude equal zero in Eq. (5) in Ref. 15. The solid curve in Fig. 6 was obtained from Eq. (6) by plotting $|X|^2$ as a function of Θ . The film was taken to be $\text{Ga}_{0.9}\text{In}_{0.1}\text{As}$. When the layer thickness is small and under the presence of a substrate crystal, the actual FWHM deviates from that calculated from Eq. (6). This is due to an additional scattering amplitude produced by the substrate at the layer Bragg angle. In Fig. 6, the FWHM ratio for a GaInAs layer with and without the GaAs substrate crystal is plotted as a function of the layer thickness for several GaInAs compositions. For the film thicknesses studied in this paper, the substrate effect in the FWHM is small and can be ignored.

V. CONCLUSION

In conclusion, we presented the lattice-relaxation data for $\text{Ga}_{1-x}\text{In}_x\text{As}$ single strained layers on GaAs(001) substrates. For samples with a thickness near the energy balance model critical thickness, major lattice relaxations occur. The Dodson-Tsao plastic flow model was used to fit the strain relaxation data for the GaInAs/GaAs system. We tentatively conclude that a more appropriate model parameter is C_1

given by Eq. (5). An approximately constant value for C_1 and different values for the dislocation source term γ_0 may fit the strain relaxation data for the GaInAs/GaAs system and the SiGe/Si system. For the films with a relaxation below the XRC sensitivity limit, the experimental rocking-curve FWHM was close to the calculated FWHM for an ideal crystal. A substantial increase in the experimental FWHM occurs when the strain relaxes beyond the XRC sensitivity limit. We discussed the experimental data on rocking-curve FWHM for the lattice-mismatched epitaxial layers, in terms of the dynamical x-ray diffraction process, the defect density depth distribution, and the theoretical FWHM of an ideal crystal.

ACKNOWLEDGMENTS

Supports for this work by the National Science Foundation under the Grant Nos. ECS-8707111 and DMR-8857403 and by the Eastman Kodak Company are gratefully acknowledged.

- ¹P. L. Gourley, I. J. Fritz, and L. R. Dawson, *Appl. Phys. Lett.* **52**, 377 (1988).
- ²I. J. Fritz, *Appl. Phys. Lett.* **51**, 1080 (1987).
- ³B. W. Dodson and J. Y. Tsao, *Appl. Phys. Lett.* **51**, 1325 (1987); *ibid.* **52**, 852(E) (1988).
- ⁴B. W. Dodson, I. J. Fritz, S. T. Picraux, and J. Y. Tsao, *Mater. Res. Soc. Symp. Proc.* **103** (1988).
- ⁵P. J. Orders and B. I. Usher, *Appl. Phys. Lett.* **50**, 980 (1987).
- ⁶D. J. Lockwood, M. W. C. Dharma-Wardana, W. T. Moore, and R. L. S. Devine, *Appl. Phys. Lett.* **51**, 361 (1987).
- ⁷For strained layer superlattices, J. W. Matthews and A. E. Blakeslee, *J. Cryst. Growth* **27**, 118 (1974); for single strained layers, J. W. Matthews, S. Mader, and T. B. Light, *J. Appl. Phys.* **41**, 3800 (1970).
- ⁸T. G. Anderson, Z. G. Chen, V. D. Kulakovski, A. Uddin, and J. T. Vallin, *Appl. Phys. Lett.* **51**, 752 (1987).
- ⁹I. J. Fritz, P. L. Gourley, and L. R. Dawson, *Appl. Phys. Lett.* **51**, 1004 (1987).
- ¹⁰C. R. Wie, H. M. Kim, and K. M. Lau, *SPIE Proc.* **877**, 41 (1988).
- ¹¹The layer thickness is the nominal film thickness from epitaxial growth parameters.
- ¹²R. People and J. C. Bean, *Appl. Phys. Lett.* **47**, 322 (1985).
- ¹³K. Kamigaki, H. Sakashita, H. Kato, M. Nakayama, N. Sano, and H. Terauchi, *Appl. Phys. Lett.* **49**, 1071 (1986).
- ¹⁴S. Takagi, *Acta Crystallogr.* **15**, 1311 (1962); D. Taupin, *Bull. Soc. Fr. Miner. Crystallogr.* **87**, 469 (1964).
- ¹⁵C. R. Wie, T. A. Tombrello, and T. Vreeland, Jr., *J. Appl. Phys.* **59**, 3743 (1986). Note: Expressions for the constants $C_{1,2}$ in Eq. (4) of this reference are in error. Correct expressions are $2 \sin(2\Theta_B)$ times those in the reference.
- ¹⁶B. W. Dodson, *Appl. Phys. Lett.* **53**, 394 (1988), and references therein.
- ¹⁷J. C. Bean, L. C. Feldman, A. T. Fiory, S. Nakahara, and I. K. Robinson, *J. Vac. Sci. Technol. A* **2**, 436 (1984).
- ¹⁸E. Kasper, H. J. Herzog, and H. Kibbel, *Appl. Phys.* **8**, 199 (1975).
- ¹⁹H. Alexander and P. Hassen, in *Solid State Physics* (Academic, New York, 1968), Vol. 22.
- ²⁰The bulk estimate for a Ge crystal of the phenomenological constant C is as large as 5.8×10^5 (Ref. 19). If the bulk parameters for GaAs are comparable to those for Ge, the fitting result for C appears to be too small. The activation energy U for the dislocation motion in GaAs is expected to be close to that of Ge which is 1.62 eV.
- ²¹V. S. Speriosu, *J. Appl. Phys.* **52**, 6094 (1981).
- ²²J. F. Chen and C. R. Wie, *J. Electron. Mater.* **17**, 501 (1988).

Journal of Applied Physics is copyrighted by the American Institute of Physics (AIP). Redistribution of journal material is subject to the AIP online journal license and/or AIP copyright. For more information, see <http://ojps.aip.org/japo/japcr/jsp>
Copyright of Journal of Applied Physics is the property of American Institute of Physics and its content may not be copied or emailed to multiple sites or posted to a listserv without the copyright holder's express written permission. However, users may print, download, or email articles for individual use.

Journal of Applied Physics is copyrighted by the American Institute of Physics (AIP). Redistribution of journal material is subject to the AIP online journal license and/or AIP copyright. For more information, see <http://ojps.aip.org/japo/japcr/jsp>